Physiological and biochemical impacts of graphene oxide in polychaetes: the case of *Diopatra neapolitana*

Lucia De Marchi, Victor Neto, Carlo Pretti, Etelvina Figueira, Luigi Brambilla, Maria Jesus Rodriguez-Douton, Francesco Rossella, Matteo Tommasini, Clascídia Furtado, Amadeu M.V.M. Soares, Rosa Freitas

PII: S1532-0456(17)30005-4
DOI: doi:10.1016/j.cbpc.2017.01.005
Reference: CBC 8277

To appear in: *Comparative Biochemistry and Physiology Part C*

Received date: 7 November 2016
Revised date: 6 January 2017
Accepted date: 17 January 2017

Please cite this article as: De Marchi, Lucia, Neto, Victor, Pretti, Carlo, Figueira, Etelvina, Brambilla, Luigi, Rodriguez-Douton, Maria Jesus, Rossella, Francesco, Tommasini, Matteo, Furtado, Clascídia, Soares, Amadeu M.V.M., Freitas, Rosa, Physiological and biochemical impacts of graphene oxide in polychaetes: the case of *Diopatra neapolitana*, *Comparative Biochemistry and Physiology Part C* (2017), doi:10.1016/j.cbpc.2017.01.005

Physiological and biochemical impacts of graphene oxide in polychaetes: the case of *Diopatra neapolitana*

Lucia De Marchi[a, b], Victor Neto[b], Carlo Pretti[c], Etelvina Figueira[a], Luigi Brambilla[d], Maria Jesus Rodriguez-Douton[e], Francesco Rossella[f], Matteo Tommasini[d], Clascídia Furtado[g], Amadeu M.V.M. Soares[a], Rosa Freitas[a *]

[a]Departamento de Biologia & CESAM, University of Aveiro 3810-193, Portugal

[b]Center for Mechanical Technology and Automation, University of Aveiro 3810-193, Portugal

[c]Department of Veterinary Sciences, University of Pisa, San Piero a Grado (PI) 56122, Italy

[d]Department of Chemistry, Materials, Chemical Enginnering "G. Natta", Politecnico di Milano, 20133 Milano, Italy

[e]Department of Pharmacy, University of Pisa, via Bonanno Pisano, 56126 Pisa, Italy

[f]NEST, Scuola Normale Superiore and Istituto Nanoscienze-CNR, 57127 Pisa, Italy

[g]Centro de Desenvolvimento da Tecnologia Nuclear, CDTN, Minas Gerais, MG, Brazil

*Corresponding Author: Rosa Freitas, Departamento de Biologia & CESAM, Universidade de Aveiro, 3810-193 Aveiro, Portugal

Mail: rosafreitas@ua.pt

Abstract

Graphene Oxide (GO) is an important carbon Nanomaterial (NM) that has been used, although limited literature is available regarding the impacts induced in aquatic organisms by this pollutant and, in particular in invertebrate species. The polychaete *Diopatra neapolitana* has frequently been used to evaluate the effects of environmental disturbances in estuarine systems due to its ecological and socio-economic importance but to our knowledge no information is available on *D. neapolitana* physiological and biochemical alterations due to GO exposure. Thus, the present study aimed to assess the toxic effects of different concentrations of GO (0.01; 0.10 and 1.00 mg/L) in *D. neapolitana* physiological (regenerative capacity) and biochemical (energy reserves, metabolic activity and oxidative stress related biomarkers) performance, after 28 days of exposure. The results obtained revealed that the exposure to GO induced negative effects on the regenerative capacity of *D. neapolitana*, with organisms exposed to higher concentrations taking longer periods to completely regenerate and less regenerated segments. GO also seemed to alter energy-related responses, especially glycogen content, with higher values in polychaetes exposed to GO which may result from a decreased metabolism (measured by electron transport system activity), when exposed to GO. Furthermore, under GO

contamination *D. neapolitana* presented cellular damage, despite higher activities of antioxidant and biotransformation enzymes in individuals exposed to GO.

Keywords: Nanomaterials, Graphene Oxide, invertebrates, body regeneration, oxidative stress

1. Introduction

Nanomaterials (NMs) are defined as materials with at least one external dimension in the size range of 1 to 100 nanometers, including nanofilms, nanowires and nanotubes or nanoparticles (Potočnik, 2011). Electromagnetic, optical, catalytic, mechanical, thermal, and pharmacokinetic properties are important characteristics of NMs. Due to these properties, NMs are increasingly being used in many different applications such as scientific, environmental, industrial, and medical, with an increase of global manufacturing products of 15% in 2015 (Renn and Roco, 2006).

Graphene, a commonly used NM, is a carbon material with sp^2-hybridized single-atom-layer structure. Few-layer graphene, graphene nanosheets and graphene oxide are related materials of graphene which can be included in graphene family materials (GFMs) (Sanchez et al., 2012). GFMs are characterized by their electronic and mechanical properties, specific magnetism, high mobility of charge carriers, high thermal conductivity, electrocatalytic activities and mechanical strength (Jastrzębska and Olszyna, 2015; Zhang et al., 2012) Graphene oxide (GO) is characterized by a structure of sp^2 carbon, oxygen, and hydrogen in variable ratios, which can be obtained by oxidizing graphite in an acidic medium (Hummers and Offeman, 1958). In GO the carbon atoms covalently bonded to oxygen containing groups are sp^3 hybrids and can disrupt the sp^2-conjugated system of graphene lattice structure (Mas-Ballesté et al., 2011). The sp^3 hybridized regions are distributed on the basal plane of graphene sheets or at the edges (Schniepp et al., 2006), making GO sheets hydrophilic, which allows them to disperse in water (Hirata et al., 2004). Chowdhury et al. (2013) investigated the aggregation kinetics and stability of GO in a water system using a wide range of aquatic chemistries (pH, salt types (NaCl, $MgCl_2$, $CaCl_2$), ionic strength) demonstrating that within approximately one month GO in natural surface water is consistently stable, indicating the potential for long-term transport of GO in the water cycle. Due to these properties, GO already demonstrated high potential for a large variety of applications (Petrone et al., 2013; Yin et al., 2014; Wang et al., 2015; Kucinskis et al., 2013; Zhang et al., 2011) Considering the increase of use and production of GFMs, and the consequent release into the environment, the toxic effects on ecosystem is becoming an urgent issue (Jastrzębska and Olszyna, 2015).

Manufactured GFMs enter the environment through intentional and unintentional releases (Klaine et al., 2008). This release can originate from wastewater treatment plants discharges, landfills and waste incineration plants, by accidental spills during production or transport of nanomaterials or from release during use (Gottschalk et al., 2015). In the environment,

organisms are able to uptake nanomaterials in different ways: direct ingestion or from contaminated prey, water filtration, inhalation, and surface contact (Cattaneo et al., 2009). Recent studies have shown that GO, but in general GFMs, are able to interact with biomolecules causing the generation of ROS (reactive oxygen species) in target cells as potential mechanism for toxicity (Sanchez et al., 2012). In fact, the extremely high hydrophobic surface area of these nanomaterials may lead to significant interactions with membrane lipids causing direct physical toxicity or adsorption of biological molecules (Sanchez et al., 2012). Therefore, the knowledge on GFMs effects and concentrations in the environment, especially in aquatic ecosystems, is an emerging issue (Klaine et al., 2008; Oberdörster et al., 2006; Zhao et al., 2014). So far concerns on GFMs toxic impact was first highlighted in Jastrzębska and Olszyna (2015) and few studies have focused on the toxicity to biota, especially on aquatic environments (Chen et al., 2012; Pretti et al., 2014). In addition, the majority of studies concerning carbon NMs impacts to aquatic organisms are focused on freshwater species (Zhou et al., 2012; Chen et al., 2012) and information about the toxicity of carbon NMs on invertebrates is even scarcer (Marques et al., 2013; Mesarič et al., 2013; Pretti et al., 2014; Al-Subiai et al., 2012). Pretti et al. (2014) showed that graphene induced oxidative stress in crustacean *Artemia salina* exposed to 1mg/L for 48h, with increasing lipid peroxidation levels and activity of antioxidant enzymes such as catalase and glutathione peroxidase. Mesarič et al. (2013), studied the possible effect of GO on cyprids (*Amphibalanus amphitrite*), and revealed that the increase of GO concentrations (1; 10; 100; 500; 750 and 1.000 mg/L) and increased exposure time (24, 48 and 72h) lead to a decrease in the swimming speed of nauplii and an increase of mortality. Al-Subiai et al. (2012) demonstrated DNA damages in mussel *Mytilus* sp. exposed to C_{60} (0.1 and 1.00 mg/L) after 3 days. Marques et al. (2013) demonstrated that nC_{60} induced oxidative stress on polychaete *Laeonereis acuta* exposed to 0.01, 0.10 and 1.00 mg/L for 24h. In fact, limited information is known on the effects of these emerging pollutants on invertebrates, especially polychaetes.

Considering the importance of polychaetes, their key role in the functioning of estuarine coastal ecosystems and their capacity to respond to stressful conditions (Dean, 2008), in the present study we investigated the biochemical and physiological alterations induced by GO in *Diopatra neapolitana* (Delle Chiaje 1841) (Annelida, Onuphidae). *D. neapolitana* is a 15–50 cm long sedentary marine polychaete that lives inside a membranous tube buried in the sediment that provides protection from disturbance and predation (Cedex, 1924). This species inhabits the intertidal mudflats of estuaries and shallow water bodies in the Atlantic, Indian Oceans (Cedex, 1924; Arias and Paxton, 2015) and Mediterranean Sea (Dağ li et al., 2005). It is already known that some polychaete species have the ability to regenerate entire or single body segments (Bely,

2006). *D. neapolitana* is able to regenerate anterior segments and prostomial structures. This species is intensively collected by bait diggers to be used as fresh fish bait (Cunha et al., 2005) and are an important food source for populations of birds, fish and other invertebrates, therefore playing an important ecological role. Previous studies already demonstrated that *D. neapolitana* is a good bioindicator of metal contamination (Freitas et al., 2012), organic matter enrichment (Carregosa et al., 2014), pharmaceutical drugs (Freitas et al., 2015), salinity shifts and pH decreases (Pires et al., 2015). However, no information is available on *D. neapolitana* impacts caused by carbon NMs, namely GO. In the present work, we used three different GO concentrations (0.01; 0.10 and 1.00 mg/L). Recently Sun et al. (2016) developed a customized dynamic probabilistic material flow model (DP-MFA) that predicted concentrations of the several Engineered NMs, in waste streams and environmental compartments, in EU by 2020. The obtained model projections showed that predicted concentrations of carbon nanotubes in surface waters are in the ng/L range (mean values of 0.97 ng/L). Compared to the concentrations tested in this study, these predicted values are three to four orders of magnitude lower than the values tested in the present study. However, other studies have already demonstrated biochemical and physiological responses on vertebrate (Kataoka et al., 2016) and invertebrate species (Pretti et al., 2014; Jastrzębska and Olszyna, 2015) at concentrations similar to the ones tested in the present study. Furthermore, effects of nanotoxicity on biological growth, cellular structure, oxidative stress, signal pathway, proteins and genes on invertebrates species, particularly on polychaetes, are still unclear (Mu et al., 2016). For these reasons, the importance of investigating the toxic effects on biological systems by these new emerging contaminates is an urgent issue to address. Furthermore, to our knowledge, no studies are known on the effect of GO on invertebrates after long-term exposure. Therefore, in the present study the biochemical and physiological alterations induced in *D. neapolitana* after 28 days exposure to GO were assessed, measuring polychaete regenerative capacity, metabolic potential, energy reserves, defense mechanisms and cellular damage.

2.Material and methods

2.1 Sampling and experimental conditions

D. neapolitana was collected in the Mira channel, the southern shallow arm of the Ria de Aveiro lagoon (Portugal). Organisms were collected in September to avoid the species reproductive period (Pires et al., 2012). After sampling, specimens were transported to the laboratory inside their tubes using plastic containers. In the laboratory, *D. neapolitana* specimens were pushed out from their tubes and placed in an aquarium for a 20 days acclimation period. The aquarium was filled with a mixture of fine and medium sediment from the sampling area (a clean sampling area with sediment median value 1.59; percentage of fines 6.75±0.79; percentage of organic matter content 3.24±0.44) (3:1) and artificial seawater (18 L, salinity 28). Salinity was set up by the addition of artificial sea salt (Tropic Marine Sea Salt) to reverse osmosis water. Temperature was maintained at 18 ± 1°C, pH ranged between 7.8 and 7.9 and photoperiod was set up at 12h light: 12h dark. During the acclimation period the aquarium was continuously aerated and organisms were fed *ad libitum* with small fragments of frozen cockles every two-three days (Pires et al., 2012). After the acclimation period, all specimens were removed from their tubes and anaesthetized with a 4% $MgCl_2.6H_2O$ solution. These organisms were then amputated at the 60^{th} chaetiger under a stereomicroscope in order to minimize the effect of body size on biochemical and physiological responses. Amputation at the 60^{th} chaetiger was selected because previous studies conducted by Pires et al. (2012) demonstrated that 100% of *D. neapolitana* individuals survived when amputated after the branchial region. After amputation, specimens were submitted to 3 different GO concentrations (0.01; 0.10 and 1.00 mg/L), plus a control (0.00 mg/L) for 28 days. Although the predicted carbon nanotubes concentrations present in surface waters revealed three to four orders of magnitude lower than GO concentrations used in the present study (Sun et al., 2016), the concentrations used were selected taking into consideration previous studies conducted with similar range of concentrations (Kataoka et al., 2016; Pretti et al., 2014; Jastrzębska and Olszyna, 2015).

For the exposure assay, three aquaria were used *per* condition, each one with 6 organisms: 3 individuals for biochemical analysis and 3 individuals for regenerative capacity evaluation. Each aquarium was filled with a mixture of fine and medium sediment from the sampling area and artificial seawater (9 L each aquarium, salinity 28) (3:1). In each aquarium the sediment layer was divided by a glass to guarantee that the individuals for regenerative capacity measurements were consistently separated from the individuals used for biochemical analysis.

This procedure ensured that, avoiding weekly removal from their tubes, no extra stress was added to the individuals used for biochemical analyses. During the experimental period organisms were submitted to constant temperature of 18 ± 1 ºC, pH between 7.8-7.9, and a photoperiod of 12:12 h (light/dark), under continuous aeration. After 28 days of exposure, organisms for biochemical analyses were frozen and the remaining individuals were maintained under the same experimental conditions until regeneration of all specimens was completed. As in the acclimation period, during the exposure period the water in aquaria was renewed every week and organisms were fed every two-three days. Furthermore, during the exposure, the GO concentrations were reestablished weekly, after every water renewal, to ensure consistent presence of GO along the experiment due to the stable solubility of GO within the water column (stable for at least 30 days (Chowdhury et al., 2013)). The hydrophilic nature of GO in seawater and the fact that the added GO was homogenously dispersed throughout the water column using one submersible circulation pump *per* aquarium diminishes the possibility that the dynamical equilibrium between gravitational settling and Brownian motion can result in the presence of NMs near the sediment–water interface (Vonk et al., 2009). The characterization of GO using a multi-technique approach were done weekly, in water samples collected immediately before medium renewal.

2.2 Laboratory analysis

Obtaining and preparation of GO solutions and characterization

GO was obtained by oxidation of natural graphite, according to the method originally proposed by Hummers and Offeman (1958) and recently modified by Marcano et al. (2010). The natural graphite analyzed by the Brazilian company Nacional de Grafite Ltda, a partner of the Instituto de Ciência e Tecnologia de Nanomateriais de Carbono/CNPq, was used as starting material for obtaining the GO. The concentrations of GO used in this study were 0.01 mg/L 0.10 mg/L and 1.00 mg/L in 9L of seawater from a stock solution of 100 mg/L concentration. Before each concentration reestablishment, the stock solution of GO was kept in an ultrasonic bath for one hour to avoid aggregation. The behavior of GO was analyzed in different water solutions: i) WP (without polychaetes) represents water samples collected from a parallel experiment conducted in a glass container filled with a mixture of fine and medium sediment from the sampling area and 600 mL of artificial seawater (salinity 28) (3:1) without polychaetes; ii) PP (with polychaetes) represents water samples collected from a parallel experiment conducted in a glass container filled with a mixture of fine and medium sediment from the sampling area and 1200 mL of artificial seawater (salinity 28) (3:1) with the presence of three polychaetes - PP

Point 1 and PP Point 2 indicate two different positions of the same PP sample which were analyzed with micro IR setup (see below); iii) GO blank solution represents water samples (salinity 28) where different GO concentrations were directly injected; iv) synthetized GO powder represents samples which have been measured directly in its original powder form.

Using a multi-techniques approach we have characterized GO powder both in the initial form and after dispersion in artificial seawater, aiming to identify its physicochemical nature as well as shedding some light on its morphology. To this purpose, GO artificial seawater dispersions were investigated using Infrared (IR) and Raman spectroscopy. The same dispersions were also drop-casted onto SiO_2/Si substrates (280 nm/400 µm) and, after drying, were investigated using scanning electron microscopy (SEM).

The GO-rich seawater samples were evaporated under vacuum at mild temperature (40°C). Upon drying, the formation of dark micrometer sized aggregates of GO flakes was observed with an optical microscope and these samples were then analysed with micro-Raman and micro-IR setups. As synthetized GO, samples were measured directly in their original powder form. This experimental approach was necessary due to the low GO concentrations used, which does not allow detection in solution state of the IR and Raman signal of GO over the solvent background. Because of the use of a microscope for IR analysis it was possible to observe the aggregates formed upon evaporation of the PP sample, at different representative spots. The IR spectra were recorded in the range 4000–650 cm^{-1} with a Nicolet ThermoElectron Continuµm IR microscope placing the solid samples in a diamond anvil cell (DAC).

Raman spectra were recorded with HORIBA-Jobin-Yvon HR800 LABRAM spectrometer using the 514.5 nm line of an Ar+ laser. The spectrometer is coupled with an Olympus BX41 optical microscope, which allows recording Raman spectra through a 50X objective. The laser power at the sample was kept at 200 µW.

SEM images were acquired using a FEG-SEM Merlin from ZEISS. Typical imaging conditions were: magnification 1-3x10^4, working distance 5-10 mm, ETH 5 kV, current 130 pA, secondary electron detector.

Physiological parameters

Mortality rate

For each condition (0.00; 0.01; 0.10 and 1.00 mg/L), the mortality rate was determined by dividing the total number of dead individuals at the end of the exposure period (28 days) by the total number of individuals used at the start of the experiment. The mortality rate was expressed as percentage.

Regenerative capacity

Nine specimens *per* condition (3 *per* aquarium) were analyzed every week until the regeneration was complete. The percentage of regenerated body part was measured, corresponding to the width of the new segments regenerated comparing with the width of the old body part, and the number of regenerated chaetigers was counted. Under microscope, regenerated chaetigers were identified by the lighter color and/or their narrower width when compared to the rest of the body. When no differences could be observed between the width of the older and the new regenerated segments the regeneration was considered complete.

Biochemical parameters

Frozen organisms (whole body) were pulverized individually with liquid nitrogen and divided in 0.3 g aliquots. A specific buffer for each biochemical analysis (1:2 w/v) was used for supernatants extraction. These samples were sonicated for 15 s at 4°C and centrifuged for 10 min at 10 000*g* (3 000*g* for electron transport system activity) at 4°C. Supernatants were stored at -80°C or immediately used to determine: glycogen content (GLY), electron transport system (ETS) activity, Lipid Peroxidation (LPO) levels, reduced (GSH) and oxidized (GSSG) glutathione content, and the activity of antioxidant (catalase, CAT; superoxide dismutase, SOD) and biotransformation (Glutathione S-transferases, GSTs) enzymes. All the biochemical parameters were performed twice. For LPO determination supernatants were extracted using 20% (v/v) trichloroacetic acid (TCA). For ETS activity quantification, supernatants were extracted in homogenizing buffer 0.1 M Tris– HCl (pH 8.5) with 15% (w/v) PVP, 153 mM magnesium sulfate ($MgSO_4$) and 0.2% (v/v) Triton X-100. GSH and GSSG contents were determined using 0.6% sulfosalicylic acid in potassium phosphate buffer (0.1 M dipotassium phosphate; 0.1 M potassium dihydrogen phosphate; 5 mM EDTA; 0.1% (v/v) Triton X-100; pH 7.5). For CAT, SOD, GSTs activities and GLY content, determination was done with potassium phosphate buffer (50 mM potassium dihydrogen phosphate; 50 mM dipotassium phosphate; 1 mM ethylenediamine tetraacetic acid disodium salt dihydrate (EDTA); 1% (v/v) Triton X-100; 1% (w/v) polyvinylpyrroli- done (PVP); 1 mM dithiothreitol (DTT)).

Energy reserves

The quantification of GLY content was done according to the sulphuric acid method (Dubois et al., 1956), using glucose standards (0-2 mg/mL). Absorbance was measured at 492 nm. The concentration of GLY was expressed in mg *per* g fresh weight (FW).

Metabolic activity

The ETS activity was measured following King and Packard (1975) method and the modifications performed by De Coen and Janssen (1997) The absorbance was measured at 490 nm during 10 min with intervals of 25 s. The amount of formazan formed was calculated using ε = 15,900 M^{-1} cm^{-1} and the results expressed in nmol/min *per* g FW.

Indicators of cellular damage

According to the method described by Ohkawa et al. (1979). LPO levels were calculated by the quantification of malondialdehyde (MDA), a by-product of lipid peroxidation. Absorbance was measured at 535 nm (ε = 156 mM^{-1} cm^{-1}) and LPO levels expressed in nmol MDA formed *per* g FW.

GSH and GSSG contents were measured at 412 nm (Rahman et al., 2014) and reagent grade GSH an GSSG were used as standards (0–60 µmol/L). GSH and GSSG were expressed in nmol *per* min *per* g FW. The GSH/GSSG was calculated dividing the GSH values by 2x the amount of GSSG.

Antioxidant enzymes activity

The activity of SOD was quantified following the method of Beauchamp and Fridovich (1971). Absorbance was measured at 560 nm. One unit of enzyme activity corresponds to a reduction of 50% of nitroblue tetrazolium (NBT). A standard curve was performed with SOD standards. Results were expressed in U *per* g FW where U corresponds to a reduction of 50% of nitroblue tetrazolium (NBT).

Formaldehyde (0-150 µM) standards were used to calculate CAT activity (Johansson and Håkan Borg, 1988). Absorbance was measured at 540 nm. Results were expressed in U per g FW were U represents the formation of 1.0 nmol formaldehyde *per* min.

Biotransformation enzymes activity

The activity of GSTs was determined following the method described by Habig et al. (1976). GSTs catalyze the conjugation of the substrate 1-chloro-2, 4-dinitrobenzene (CDNB) with glutathione, forming a thioeter. Absorbance was measured at 340 nm and the activity of GSTs was determined using the extinction coefficient of 9.6 mM cm^{-1} for CDNB. Results were expressed in U *per* g FW were U is defined as the amount of enzyme that catalysis the formation of 1 µmol of dinitrophenyl thioether *per* min.

2.3 Data analysis

The regenerative capacity (percentage of regenerated body width and the number of new chaetigers at the end of the regeneration) and the biochemical descriptors (GLY, ETS, LPO, CAT, SOD, GSTs, GSH/GSSG measured after 28 days of exposure) were submitted to hypothesis testing using permutational multivariate analysis of variance with the PERMANOVA+ add-on in PRIMER v6. A one-way hierarchical design was followed in this analysis. The pseudo-F values in the PERMANOVA main tests were evaluated in terms of significance. Significant differences were observed using main test and consequently pairwise comparisons were performed. The t-statistics in the pairwise comparisons were evaluated in terms of significance. Values lower than 0.05 were considered as significantly different. The null hypothesis tested was: for each biomarker, no significant differences exist among exposure concentrations.

The matrix gathering the biomarker responses *per* exposure concentration was used to calculate the Euclidean distance similarity matrix. This similarity matrix was simplified through the calculation of the distance among centroids matrix based on GO concentrations, which was then submitted to ordination analysis, performed by Principal Coordinates (PCO). Pearson correlation vectors of regenerative and biochemical descriptors (correlation >0.75) were provided as supplementary variables being superimposed on the PCO graph.

3. Results

3.1 Characterization GO

Characterization results at the beginning (end of the first week) and end (fourth week) of the experiment are presented in Figures 1 and 2.

In Figure 1A we report the IR spectrum of synthetized GO which displays several spectral features: a broad band centered at 3450 cm^{-1} (assigned to the stretching of OH groups); a medium intensity band near 1720 cm^{-1} (assigned to the stretching of carbonyl bonds); a strong structured band peaking at 1580 cm^{-1} (assigned to the stretching of polarized C=C bonds) with a shoulder at 1620 cm^{-1} (assigned to the carboxylic CO stretching); a broad and structured feature ranging from 1400 cm^{-1} to 1000 cm^{-1} whose most prominent peak at 1240 cm^{-1} is assigned to the antisymmetric stretching vibrations of the C-O-C moieties. All these bands originate from oxygen bearing functional groups attached to the C=C sp^2 network of GO and provide a characteristic spectral pattern usually observed in this class of materials (Marcano et al., 2010; Shen et al., 2009; Acik et al., 2010; Agorku et al., 2015). Particularly our results are in agreement with study conducted by Jastrzębska et al. (2016) who showed all these types of vibrations occurred in pure GO.

Differently from synthetized GO and GO blank solution, the IR spectra of GO artificial seawater dispersions (PP) showed a more complex pattern (Figure 1B). Two different regions of the PP sample were analyzed with the micro-IR setup. Point 1 displayed evidence of inorganic species, such $CaCO_3$ (strong band at 1440 cm^{-1}). Point 2 showed a sizeable organic fraction, with characteristic –NH, amide I and amide II bands vibrations associated to proteins. This is not surprising if we take into account that a large number of chemical compounds can be present in sediment (percentage of organic matter content 3.24±0.44), together with residuals of the *D. neapolitana* itself. Due to the chemical complexity of these samples, the use of their IR spectra for quantitative GO analysis is difficult. In this scenario, Raman spectroscopy may play a beneficial role since, through resonance enhancement, it just displays signals originating from the π-conjugated sp^2 fraction of GO.

In Figure 1C representative Raman spectra of different samples measured with a micro-Raman setup in the range 1000-1900 cm^{-1} are reported. The evident G and D Raman lines (respectively located at 1591 and 1343 cm^{-1}) confirm the presence of GO in all samples. The G line is associated to the collective ring stretching vibrations of a graphitic layer (Kudin et al., 2007; Marcano et al., 2010; Shen et al., 2009). The D line is related to collective ring breathing

vibrations of condensed benzene rings associated to finite graphitic domains in GO. The relative intensity of the D line with respect to the G line (I_D/I_G) carries information on the degree of defects in the sample compared to a perfect graphene layer (for which $I_D/I_G = 0$). On the other hand, the rather large Full Width at Half Maximum (FWHM) of the G and D lines (about 100 cm^{-1}) reflects the disordered nature of GO. The Raman spectra reported in Figure 1C are very similar, indicating that the sp^2 fraction of the GO structures is fairly stable under the different experimental conditions considered in this study and are similar to those found in literature (Jastrzębska et al., 2016).

IR and Raman spectroscopy undoubtedly reveal the presence of GO in our samples but these techniques do not provide any information concerning the morphology-average shape and size-of the GO crystallites. This key issue was fully addressed using SEM. In Figure 2, SEM images of the GO artificial seawater dispersions drop-casted onto SiO_2/Si substrates are presented. In particular, the frequent occurrence of structures with dimensions well sub-micron is highlighted (cf. Figure 2, A-B, white arrows), which display a feeble contrast in respect to the insulating 280 nm thick silicon oxide layer underneath. The larger crystals that can be seen in Figure 2 are NaCl crystals that crystallized during seawater evaporation. Studies conducted by Chowdhury et al. (2013), which investigated the aggregation kinetics and stability of GO using time-resolved dynamic light scattering (DLS) over a wide range of aquatic chemistry (pH, salt types (NaCl, $MgCl_2$, $CaCl_2$), showed that only $CaCl_2$ destabilized GO compared to the reaming salt types, indicating that NaCl should have minor influence on the fate of the nominal concentrations of GO used in the present work.

A closer look to these nanostructures (cf. Figure 2, C-E) reveals their dimensions and morphology: (i) the GO "flakes" have a typical lateral size of 200-400 nm, (ii) their edges display well defined angles, and (iii) the weak contrast suggests a thickness of the order of several atomic layers. Altogether, these experimental evidences demonstrate a profusion of nanoscale GO crystallites into our GO artificial seawater dispersions.

3.2 Physiological parameters

Mortality rate

Individuals exposed to 0.01 and 0.10 mg/L showed 11% mortality, with significant differences to individuals exposed to control and 1.00 mg/L. *D. neapolitana* exposed to 1.00 mg/L showed significantly higher mortality (22%) compared to the remaining conditions. At control (0.00 mg/L) 100% of survival was recorded after exposure.

Regenerative capacity

The mean values for the regenerated body, measured as the percentage of body width regenerated, and the number of chaetigers regenerated after 11, 18, 25, 32, 39, 46, 53 and 60 days are presented in Table 1 and illustrated in Figure 3. Table 1 also indicates, for all the conditions, the mean number of days that the organisms needed to completely regenerate the missing body part and the total number of new chaetigers regenerated after complete regeneration. After amputation, at the 11th all individuals were healing the cut region (Table 1). Eighteen days after amputation, all specimens were regenerating a small reddish differentiated portion with rudimentary anal cirri without significant differences among conditions. During the course of the experiment, differences between exposed and non-exposed individuals to different GO concentrations became more noticeable (Table 1). At day 25 no significant differences were observed among conditions regarding the percentage of regenerated body but in terms of number of new chaetigers significant differences were observed between specimens exposed to 1.00 mg/L (0 chaetigers) and organisms exposed to the remaining concentrations (Table1, Figure 3). The specimens from control showed the highest number of new chaetigers but significant differences were only observed in comparison to specimens exposed to the highest concentration (1.00 mg/L) (Table1, Figure 3). Significant differences in terms of percentage of regenerated body were noticeable at day 32 between individuals from control (higher percentage of regenerated body) and individuals exposed to 1.00 mg/L but no significant differences were found among individuals from the remaining concentrations (0.01 and 0.10 mg/L). Considering the number of new chaetigers, significant differences were only found between organisms under control conditions and 1.00 mg/L. At day 39, the percentage of regenerated body and number of new chaetigers were significantly higher in individuals from the control and exposed to the lowest GO concentration (0.01 mg/L) compared to individuals exposed to higher concentrations (0.10 mg/L and 1.00) (Table 1). Significantly lower percentage of regenerated body was found in individuals from the highest GO concentrations (0.10 and 1.00 mg/L) and control condition 46 days after amputation. Concerning the number of regenerated segments, after 46 days, individuals from the two higher concentrations (0.10 and 1.00 mg/L) regenerated significantly fewer chaetigers than individuals exposed to control condition and the lowest GO (0.01 mg/L). At days 53 and 60, specimens from the control were able to regenerate significantly higher percentage of body compared with all the reaming conditions, but no significant differences were found between individuals from 0.01 and 0.10 mg/L GO as well between individuals from 0.10 and 1.00 mg/L (Table 1, Figure 3). Nevertheless, significant differences were observed between individuals at the lowest (0.01 mg/L) and highest (1.00 mg/L) GO exposures. In terms of number

of new chaetigers, at day 53, individuals from control showed a significantly higher number of new chaetigers compared with the remaining conditions, followed by organisms exposed to 0.01 mg/L GO (with significant differences compared to the other conditions) (Table 1, Figure 3). Lower number of new chaetigers was observed in individuals exposed to 0.10 and 1.00 mg/L, with no significant differences between both conditions. At the 60th day, significant differences in terms of new chaetigers were observed between individuals from control and from 0.01 mg/L and organisms exposed to higher GO concentrations (0.10 and 1.00 mg/L). Significant differences were also found between organisms exposed to 0.10 and 1.00 mg/L, with less new chaetigers in individuals exposed to 1.00 mg/L (Table 1). The results further reveled that control organisms completely regenerated after 62 days (62.00±1.73), while specimens exposed to 0.01 mg/L of GO completed the regeneration after 68 days (68.50± 1.51), organisms exposed to 0.10 mg/L needed 76 days to completely regenerate (76.12±2.23) and polychaetes exposed to 1.00 mg/L of GO took a significantly longer time to completely regenerate (85.28 ±3.63 days) (Table 1). Considering the total number of chaetigers regenerated the present study showed that with increasing GO concentrations specimens tended to regenerate fewer new chaetigers, with individuals under control presenting the highest number of new chaetigers (38.44±4.03) while under the highest GO concentration polychaetes regenerated fewer chaetigers (22.57±5.38) (Table 1).

3.3 Biochemical responses

Energy reserves

Alterations in GLY content are presented in Figure 4A. Results showed higher GLY content in organisms exposed to GO in comparison with organisms under control, with the highest values in polychaetes exposed to 0.10 mg/L of GO. Significant differences were observed between organisms exposed to control and organisms exposed to 0.10 and 1.00 mg/L of GO.

Metabolic activity

The results on ETS activity (Figure 4B) revealed a decreasing trend with the increase of exposure concentration, but no significant differences were observed among organisms exposed to different conditions.

Indicators of cellular damage

Concerning cellular damage the results obtained revealed that *D. neapolitana* presented an

increase of LPO levels with the increase of GO concentrations, with the highest values at the highest GO concentration (1.00 mg/L) (Figure 5A). Significantly lower LPO values were found in individuals from control in comparison with organisms from the remaining conditions as well as between individuals at the lowest (0.01 mg/L) and the highest (1.00 mg/L) GO concentrations (Figure 5A).

The ratio between reduced (GSH) and oxidized (GSSG) glutathione showed that organisms presented lower GSH/GSSG values under GO compared to specimens under control (Figure 5B). Along the exposure gradient *D. neapolitana* presented decreased GSH/GSSG with significantly lower values at the highest GO concentration (1.00 mg/L) compared to control.

Antioxidant enzymes activity

The activity of SOD (Figure 6A) increased in organisms exposed to GO, with significant differences between individuals exposed and non-exposed to GO. The highest SOD activity was obtained at an intermediate concentration (0.10 mg/L), with significant differences to the remaining conditions. No statistical differences were observed in SOD activity between individuals exposed to the lowest (0.01 mg/L) and the highest (1.00 mg/L) concentrations.

The activity of CAT (Figure 6B) demonstrated that this enzyme tended to increase with the increase of GO concentration, with significant differences between individuals exposed to the two highest exposure concentrations (0.10 and 1.00 mg/L), between organisms under the highest and the two lowest (0.01 mg/L and control) concentrations, as well as between organisms under 0.10 mg/L and control conditions (Figure 6B).

Biotransformation enzyme activity

The activity of GSTs (Figure 6C) showed higher values in organisms exposed to GO, with significantly lower values in individuals at control compared to specimens under the remaining conditions. Significant differences were also observed between organisms exposed to the highest concentration (1.00 mg/L) and organisms under the remaining conditions (Figure 6C). No significant differences were found between organisms under intermediate concentrations (0.01 and 0.10 mg/L) (Figure 6C).

3.4 Multivariate analysis

In Figure 7 the centroid PCO ordination graph is represented resulting from multivariate analysis applied to the physiological and biochemical parameters. The PCO axis 1 explained 81.3% of total data variation, separating control (0.00) and the lowest exposure concentration

(0.01 mg/L) at the negative side, from 0.10 and 1.00 mg/L at the positive side. The PCO axis 2 explained 16.1% of total data variation, separating the highest concentration (1.00 mg/L) and control (0.00) (in the positive side of the axis) from 0.01 and 0.10 mg/L conditions (at the negative side of the axis). The polychaetes exposed in control and the lowest exposure concentration were characterized by higher number of new chaetigers, higher ETS and GSH/GSSG values; polychaetes exposed to 0.10 mg/L were associated to higher GLY content and SOD values; and polychaetes under the highest GO concentration (1.00 mg/L) were well correlated to higher LPO, CAT and GSTs values and higher number of days needed to complete regenerate.

4. Discussion

The present study showed the toxic impacts induced by GO on *D. neapolitana*, a widespread polychaete species in the world (Dean, 2008). Although studies on GFMs toxicity have been recently published (Jastrzębska et al., 2012; Liu et al., 2009), GO has not been the object of exhaustive investigations concerning the risks that it may pose to the aquatic environment and, especially on inhabiting organisms (Mesarič et al., 2013; Chang et al., 2011). Furthermore, since the majority of the literature on NMs impacts on marine invertebrates is based on acute exposures, that are not sufficient to allow for a potential acclimation to a new environment or may not induce responses, a 28 days experiment was carried out allowing to assess the physiological and biochemical alterations provoked by different GO concentrations. The present study showed that after exposure, higher mortality was recorded in organisms exposed to the highest GO concentration compared to the remaining conditions. These results are in agreement with previous studies on GO toxicity. Mesarič et al. (2013) demonstrated that single-layer GO had negative impacts on settlement, mortality and swimming behaviour of *A. amphitrite* nauplii after 24, 48, and 72 h exposure to 1; 10; 100; 500; 750 and 1.000 mg/L. Chang et al. (2011) investigated the influence of GO on morphology, viability, mortality and membrane integrity of A549 cells at different concentrations (10, 25, 50, 100 and 200 mg/L) for 48 h showing that the highest GO dose induced decrease of cell viability.

The present study clearly demonstrated that GO has a negative effect on the regenerative capacity of *D. neapolitana*, with less chaetigers regenerated and longer regeneration period in individuals exposed to the highest concentration. Although several authors already demonstrated that the regenerative capacity of *D. neapolitana* is affected by different stressors (pharmaceutical drugs (Freitas et al., 2015), organic matter (Carregosa et al., 2014), salinity and temperature (Pires et al., 2015)), the present study is the first revealing the impacts of GO on this physiological parameter in polychaetes. Nevertheless, previous studies showed that carbon based NMs induce alterations in physiological functions in invertebrate species (Wu et al., 2013; Mesarič et al., 2015). In the nematode *Caenorhabditis elegans* Wu et al. (2013) examined the potential impacts of GO comparing *in vivo* effects between acute and chronic exposures, and found that prolonged exposure to 0.5–100 mg/L caused damage on functions of both primary (intestine), and secondary (neuron and reproductive organ) targeted organs. Moschino et al. (2014) demonstrated the toxicity of SWCNH (Single walled carbon nanohorns) on polychaete, *Hediste diversicolor* and mussel *Mytilus galloprovincialis*. Mussels and polychaetes were exposed to three SWCNH concentrations: 1, 5, and 10 mg/L 24 and 48h and the authors revealed

sub-lethal effects at the digestion level with a possible less efficient intracellular digestive process. Mesarič et al. (2015) investigated the effects of carbon black, GO, and multiwall carbon nanotubes on *A. salina* larvae for 48h, and showed that these nanomaterials were present in the gut, and attached onto the body surface of the organisms causing a concentration–dependent inhibition of larval swimming.

Our findings further demonstrate that GO induced biochemical alterations in *D. neapolitana*. Polychaetes presented significantly higher GLY content when under GO concentrations in comparison to control. These results may indicate that individuals under GO exposure may prevent energy expenditure, namely in the regeneration process (which was strongly affected), increasing the content of this energy reserve. In fact, in the present study individuals under control condition presented the highest ETS activity, which suggests a higher metabolic rate leading to a higher expenditure of energy reserves, as observed by the lowest GLY content at this condition. This capacity was decreased at the highest GO concentrations (1.00 mg/L) which may indicate that at high levels of GO polychaetes reduce their metabolic capacity resulting in the increase of energy reserves storage. Previous studies already demonstrated that some polychaete species under certain conditions may decrease their metabolism and, therefore, reduce energy expenditure (Carregosa et al., 2014; Maranho et al., 2014; Fossi Tankoua et al., 2012). Maranho et al. (2014) showed an increase of energy reserves with increasing concentrations of the antiepileptic drug carbamazepine (CBZ) in *H. diversicolor*. Tankoua et al. (2012) demonstrated that, for the same polychaete species, in a contaminated site (Loire estuary, France) the energy reserves of the organisms were higher compared to the organisms from a cleaner site (Bay of Bourgneuf, France). Also, studies conducted Carregosa et al. (2014) revealed that *D. neapolitana* increased GLY content under stressful organic matter enrichment conditions.

Our findings further demonstrated that GO induced oxidative stress in *D. neapolitana*, evidenced by an increase of LPO and the inability of antioxidant and biotransformation mechanisms to prevent such membrane damage. In particular, although antioxidant and biotransformation mechanisms were enhanced in contaminated organisms, these defenses were not enough to prevent cellular damage caused by GO in *D. neapolitana*. The present data demonstrated an increase of LPO levels with the increase of GO concentrations, with the highest values at the highest GO concentration (1.00 mg/L). Also, with the increasing exposure concentrations the ratio GSH/GSSG strongly decreased, a pattern that indicates the development of oxidative stress in organisms. It has already been demonstrated that oxidative stress is generated by various nanoparticles (Li et al., 2008; Yang et al., 2008) and that GO induces ROS

generation, even at low concentrations (Chang et al., 2011). The generation of ROS and an increase of Lactate dehydrogenase (LDH) release for example, were already shown in *C. elegans* after the acute exposure to GO at concentrations of 10–100 mg/L (Wu et al., 2013). Nevertheless, to our knowledge no studies have yet reported the induction of oxidative stress in polychaete species due to GO. Previous studies already reported the induction of oxidative stress in *D. neapolitana* due to different contaminants. Freitas et al. (2015) revealed cellular damage induced by CBZ, showing that this drug induced LPO in *D. neapolitana* with a decrease in the GSH/GSSG ratio. Carregosa et al. (2014) showed a significant increase in LPO in *D. neapolitana* from areas with higher organic matter. Besides LPO alterations, results on the antioxidant enzyme SOD revealed that the activity of this enzyme was significantly increased in organisms exposed to GO compared to non-contaminated organisms. These results are in agreement with the study conducted by Wu et al. (2013) suggesting that the induction of oxidative stress due to GO may be associated with the alteration of SOD activity. However, in the present study, the highest SOD activity was observed at an intermediate concentration (0.10 mg/L) decreasing at the highest GO concentration. This fact may indicate that SOD was actively involved in ROS elimination at lower concentrations (0.01 and 0.10 mg/L), but above a certain level of stress (as observed at the highest GO concentration) this enzyme reduced its efficiency to eliminate ROS, leading to the induction of LPO at higher GO concentrations. This may be due to less activity of the enzymes or lower number of enzymes. Also Contardo-Jara et al. (2011) found a decrease in the activity of SOD in the mussel *Dreissena polymorpha* exposed to the highest drug (CBZ) concentration (236 mg/L). A similar pattern was found by Freitas et al. (2015), that suggested that higher LPO levels in *D. neapolitana* exposed to CBZ could be explained by the fact that SOD and CAT were not able to act efficiently as antioxidant defense, which was at least partially responsible for increased LPO. Concerning CAT, in the present study the activity of this enzyme was also significantly higher in organisms exposed to GO concentrations. Although to our knowledge no studies evaluated effects provoked in CAT and SOD enzymes in polychaetes after exposure to GO, recently Pretti et al. (2014) showed that, graphene monolayer flakes up to the concentration of 1mg/L induced increased activity of CAT in *Artemia salina* after 48h exposure. On the other hand, Mesarič et al. (2015) showed for the same species that exposure to carbon black, GO, and MWCNT after 48h did not induce significant differences in CAT activity at any of the tested concentrations. In the present study the activity of GSTs showed higher values at all GO exposure concentrations compared to control. To date, few studies on GSTs activities are available for polychaete exposure to NMs (Marques et al., 2013; Galloway et al., 2010) and no data referring to carbon NMs with

particularly attention on GO exposure. However, with the same species *D. neapolitana*, Carregosa et al. (2014) demonstrated an increase of GSTs activity with the increase of organic matter content, and other authors showed that the activity of GSTs in the polychaete species *H. diversicolor* increased in polluted sites from the SW Spain (Pérez et al., 2004; Solé et al., 2009), the Sado estuary, Portugal (Moreira et al., 2006), and the Seine estuary, France (Durou et al., 2007).

Conclusion

The present study demonstrated that regeneration in *D. neapolitana* was retarded as the number of newly regenerated segments was diminished in individuals exposed to GO. Since organisms presented higher LPO levels when exposed to GO concentrations, the reduction of the ability to regenerate a new body portion could be due to oxidative stress, as free radicals may cause damaging effects on the biochemical and cellular functions that underlie the regenerative process. Higher enzymatic activities and LPO levels detected in individuals exposed to GO concentrations suggest that the defense mechanisms were in part unable to eliminate ROS and prevent deleterious effects on membrane lipids leading to LPO.

In summary, *D. neapolitana* was negatively impacted by GO, with physiological and biochemical impairments induced by these carbon NM, indicating that this species can be used as bioindicator to monitor environmental pollution related to carbon based NMs pollution. Nevertheless, further research is needed to verify and quantify the possible uptake of GO by these organisms. As this topic of research develops and more information is available regarding realistic GO concentrations that marine invertebrates may be exposed to, it will be necessary to modify and limit the range of GO concentrations to represent contaminated sites and perform new toxicity tests.

Acknowledgements

This work was supported by CESAM (UID/AMB/50017), to FCT/MEC through national funds, and the co-funding by the FEDER, within the PT2020 Partnership Agreement and Compete 2020. Lucia De Marchi benefited from PhD grant (SFRH/BD/101273/2014) and Rosa Freitas benefited from a post-doc grant (SFRH/BPD/92258/2013) given by the Portuguese FCT.

References

Acik, M., Lee, G., Mattevi, C., Chhowalla, M., Cho, K., Chabal, Y.J., 2010. Unusual infrared-

absorption mechanism in thermally reduced graphene oxide. *Nat. Mater.* 9, 840–845. doi:10.1038/nmat2858

Agorku, E.S., Mamo, M.A., Mamba, B.B., Pandey, A.C., Mishra, A.K., 2015. Palladium-decorated zinc sulfide/reduced graphene oxide nanocomposites for enhanced visible light-driven photodegradation of indigo carmine. *Mater. Sci. Semicond. Process*. 33, 119–126. doi:10.1016/j.mssp.2015.01.033

Al-Subiai, S.N., Arlt, V.M., Frickers, P.E., Readman, J.W., Stolpe, B., Lead, J.R., Moody, a J., Jha, A.N., 2012. Merging nano-genotoxicology with eco-genotoxicology: an integrated approach to determine interactive genotoxic and sub-lethal toxic effects of C(60) fullerenes and fluoranthene in marine mussels, *Mytilus* sp. *Mutat. Res.* 745, 92–103. doi:10.1016/j.mrgentox.2011.12.019

Arias, A., Paxton, H., 2015. *Onuphis* and *Aponuphis* (Annelida: Onuphidae) from southwestern Europe, with the description of a new species. 3949, 345–369.

Beauchamp, C., Fridovich, I., 1971. Superoxide dismutase: improved assays and an assay applicable to acrylamide gels. *Anal. Biochem.* 44, 276–287.

Bely, A.E., 2006. Distribution of segment regeneration ability in the Annelida. *Integr. Comp. Biol.* 46, 508–518. doi:10.1093/icb/icj051

Carregosa, V., Velez, C., Pires, A., Soares, A.M.V.M., Figueira, E., Freitas, R., 2014. Physiological and biochemical responses of the Polychaete *Diopatra neapolitana* to organic matter enrichment. *Aquat. Toxicol.* 155, 32–42. doi:10.1016/j.aquatox.2014.05.029

Cattaneo, A.G., Gornati, R., Bernardini, G., 2009. Ecotoxicology of nanomaterials□: the role of invertebrate testing Abstract Engineered nanomaterials represent a new and expanding class of chemicals whose environmental hazard is actually poorly determined . The peculiar behavior of nanomaterials makes th 78–97.

Cedex, B.P.P., 1924. Faune de France 5: Polychètes errantes. *Nature* 113, 528–529. doi:10.1038/113528b0

Chang, Y., Yang, S.-T., Liu, J.-H., Dong, E., Wang, Y., Cao, A., Liu, Y., Wang, H., 2011. In vitro toxicity evaluation of graphene oxide on A549 cells. *Toxicol. Lett.* 200, 201–10. doi:10.1016/j.toxlet.2010.11.016

Chen, D., Feng, H., Li, J., 2012. Graphene oxide: Preparation, functionalization, and electrochemical applications. *Chem. Rev*. doi:10.1021/cr300115g

Chen, L., Hu, P., Zhang, L., Huang, S., Luo, L., Huang, C., 2012. Toxicity of graphene oxide and multi-walled carbon nanotubes against human cells and zebrafish. *Sci. China Chem.* 55, 2209–2216. doi:10.1007/s11426-012-4620-z

Chowdhury, I., Duch, M.C., Mansukhani, N.D., Hersam, M.C., Bouchard, D., 2013. Colloidal properties and stability of graphene oxide nanomaterials in the aquatic environment. *Environ. Sci. Technol.* 47, 6288–6296. doi:10.1021/es400483k

Contardo-Jara, V., Lorenz, C., Pflugmacher, S., Nützmann, G., Kloas, W., Wiegand, C., 2011. Exposure to human pharmaceuticals Carbamazepine, Ibuprofen and Bezafibrate causes molecular effects in *Dreissena polymorpha*. *Aquat. Toxicol.* 105, 428–437. doi:10.1016/j.aquatox.2011.07.017

Cunha, T., Hall, A., Queiroga, H., 2005. Estimation of the *Diopatra neapolitana* annual harvest resulting from digging activity in Canal de Mira, Ria de Aveiro. *Fish. Res.* 76, 56–66. doi:10.1016/j.fishres.2005.05.008

Dağ li, E., Ergen, Z., Çinar, M.E., 2005. One-year observation on the population structure of *Diopatra neapolitana* Delle Chiaje (Polychaeta: Onuphidae) in Izmir Bay (Aegean sea, eastern Mediterranean). *Mar. Ecol.* 26, 265–272.

De Coen, W., Janssen, C.R., 1997. The use of biomarkers in *Daphnia magna* toxicity testing. IV.Cellular Energy Allocation: a new methodology to assess the energy budget of toxicant-stressed *Daphnia* populations. *J. Aquat. Ecosyst. Stress Recover.* 6, 43–55. doi:10.1023/A:1008228517955

Dean, H., 2008. The use of polychaetes (Annelida) as indicator species of marine pollution: a review. *Rev Biol Trop* 56, 11–38.

Dubois, M., Gilles, K. a., Hamilton, J.K., Rebers, P. a., Smith, F., 1956. Colorimetric method for determination of sugars and related substances. *Anal. Chem.* 28, 350–356. doi:10.1021/ac60111a017

Durou, C., Poirier, L., Amiard, J.C., Budzinski, H., Gnassia-Barelli, M., Lemenach, K., Peluhet, L., Mouneyrac, C., Roméo, M., Amiard-Triquet, C., 2007. Biomonitoring in a clean and a multi-contaminated estuary based on biomarkers and chemical analyses in the endobenthic worm *Nereis diversicolor*. *Environ. Pollut.* 148, 445–458. doi:10.1016/j.envpol.2006.12.022

Fossi Tankoua, O., Buffet, P.E., Amiard, J.C., Amiard-Triquet, C., Méléder, V., Gillet, P., Mouneyrac, C., Berthet, B., 2012. Intersite variations of a battery of biomarkers at different levels of biological organisation in the estuarine endobenthic worm *Nereis diversicolor* (Polychaeta, Nereididae). *Aquat. Toxicol.* 114–115, 96–103. doi:10.1016/j.aquatox.2012.02.016

Freitas, R., Almeida, Â., Pires, A., Velez, C., Calisto, V., Schneider, R.J., Esteves, V.I., Wrona, F.J., Figueira, E., Soares, A.M.V.M., 2015. The effects of carbamazepine on

macroinvertebrate species: Comparing bivalves and polychaetes biochemical responses. *Water Res.* 85, 137–47. doi:10.1016/j.watres.2015.08.003

Freitas, R., Pires, A., Quintino, V., Rodrigues, A.M., Figueira, E., 2012. Subcellular partitioning of elements and availability for trophic transfer: Comparison between the Bivalve *Cerastoderma edule* and the Polychaete *Diopatra neapolitana*. *Estuar. Coast. Shelf Sci.* 99, 21–30. doi:10.1016/j.ecss.2011.11.039

Galloway, T., Lewis, C., Dolciotti, I., Johnston, B.D., Moger, J., Regoli, F., 2010. Sublethal toxicity of nano-titanium dioxide and carbon nanotubes in a sediment dwelling marine polychaete. *Environ. Pollut.* 158, 1748–1755. doi:10.1016/j.envpol.2009.11.013

Gottschalk, F., Lassen, C., Kjoelholt, J., Christensen, F., Nowack, B., 2015. Modeling flows and concentrations of nine engineered nanomaterials in the Danish environment. *Int. J. Environ. Res. Public Health* 12, 5581–602. doi:10.3390/ijerph120505581

Habig, W.H., Pabst, M.J., Jakoby, W.B., 1976. Glutathione S-transferase AA from rat liver. *Arch. Biochem. Biophys.* 175, 710–716. doi:10.1016/0003-9861(76)90563-4

Hirata, M., Gotou, T., Horiuchi, S., Fujiwara, M., Ohba, M., 2004. Thin-film particles of graphite oxide 1: High-yield synthesis and flexibility of the particles. *Carbon N. Y.* 42, 2929–2937. doi:10.1016/j.carbon.2004.07.003

Hummers, W.S., Offeman, R.E., 1958. Preparation of Graphitic Oxide. *J. Am. Chem. Soc.* 80, 1339–1339. doi:10.1021/ja01539a017

Jastrzębska A.M., Karcz, J., Letmanowski, R., Zabost, D., Ciecierska, E., Siekierski, M., Olszyna, A., 2016. Synthesis of RGO/TiO_2 nanocomposite flakes and characterization of their unique electrostatic properties using zeta potential measurements. *J. Alloys Compd.* 679, 470–484. doi:10.1016/j.jallcom.2016.04.043

Jastrzębska, A.M., Kurtycz, P., Olszyna, A.R., 2012. Recent advances in graphene family materials toxicity investigations. *J. Nanopart. Res.* 14, 1320. doi:10.1007/s11051-012-1320-8

Jastrzębska, A.M., Olszyna, A.R., 2015. The ecotoxicity of graphene family materials: current status, knowledge gaps and future needs. *J. Nanoparticle Res.* 17, 40. doi:10.1007/s11051-014-2817-0

Johansson, L.H., Håkan Borg, L.A., 1988. A spectrophotometric method for determination of catalase activity in small tissue samples. *Anal. Biochem.* 174, 331–336. doi:10.1016/0003-2697(88)90554-4

Kataoka, C., Nakahara, K., Shimizu, K., Kowase, S., Nagasaka, S., Ifuku, S., Kashiwada, S., 2016. Salinity-dependent toxicity of water-dispersible, single-walled carbon nanotubes to

Japanese medaka embryos. *J. Appl. Toxicol.* doi:10.1002/jat.3373

King, F.D., Packard, T.T., 1975. Respiration and the activity of the respiratory electron transport system in marine zooplankton. *Limnol. Oceanogr.* 20, 849–854. doi:10.4319/lo.1975.20.5.0849

Klaine, S.J., Alvarez, P.J.J., Batley, G.E., Fernandes, T.F., Handy, R.D., Lyon, D.Y., Mahendra, S., McLaughlin, M.J., Lead, J.R., 2008. Nanomaterials in the environment: behavior, fate, bioavailability, and effects. *Environ. Toxicol. Chem.* 27, 1825–1851. doi:10.1897/08-090.1

Kucinskis, G., Bajars, G., Kleperis, J., 2013. Graphene in lithium ion battery cathode materials: A review. *J. Power Sources* 240, 66–79. doi:10.1016/j.jpowsour.2013.03.160

Kudin, K.N., Ozbas, B., Schniepp, H.C., Prud'homme, R.K., Aksay, I. a, Car, R., 2007. Raman spectra of graphite oxide and functionalized graphene sheets. *Nano Lett.* 8, 36–41. doi:10.1021/nl071822y

Li, N., Xia, T., Nel, A.E., 2008. The role of oxidative stress in ambient particulate matter-induced lung diseases and its implications in the toxicity of engineered nanoparticles. *Free Radic. Biol. Med.* 44, 1689–1699. doi:10.1016/j.freeradbiomed.2008.01.028

Liu, Z., Tabakman, S., Welsher, K., Dai, H., 2009. Carbon Nanotubes in Biology and Medicine: In vitro and in vivo Detection, Imaging and Drug Delivery. *Nano Res.* 2, 85–120. doi:10.1007/s12274-009-9009-8

Maranho, L. a, Baena-Nogueras, R.M., Lara-Martín, P. a, DelValls, T. a, Martín-Díaz, M.L., 2014. Bioavailability, oxidative stress, neurotoxicity and genotoxicity of pharmaceuticals bound to marine sediments. The use of the polychaete *Hediste diversicolor* as bioindicator species. *Environ. Res.* 134, 353–65. doi:10.1016/j.envres.2014.08.014

Marcano, D.C., Kosynkin, D. V., Berlin, J.M., Sinitskii, A., Sun, Z., Slesarev, A., Alemany, L.B., Lu, W., Tour, J.M., 2010. Improved synthesis of graphene oxide. *ACS Nano* 4, 4806–4814. doi:10.1021/nn1006368

Marques, B.F., Cordeiro, L.F., Kist, L.W., Bogo, M.R., López, G., Pagano, G., Muratt, D.T., de Carvalho, L.M., Külkamp-Guerreiro, I.C., Monserrat, J.M., 2013. Toxicological effects induced by the nanomaterials fullerene and nanosilver in the polychaeta *Laeonereis acuta* (Nereididae) and in the bacteria communities living at their surface. *Mar. Environ. Res.* 89, 53–62. doi:10.1016/j.marenvres.2013.05.002

Mas-Ballesté, R., Gómez-Navarro, C., Gómez-Herrero, J., Zamora, F., 2011. 2D materials: to graphene and beyond. *Nanoscale* 3, 20–30. doi:10.1039/c0nr00323a

Mesarič, T., Gambardella, C., Milivojević, T., Faimali, M., Drobne, D., Falugi, C., Makovec, D., Jemec, A., Sepčić, K., 2015. High surface adsorption properties of carbon-based

nanomaterials are responsible for mortality, swimming inhibition, and biochemical responses in *Artemia salina* larvae. *Aquat. Toxicol.* 163, 121–9. doi:10.1016/j.aquatox.2015.03.014

Mesarič, T., Sepčič, K., Piazza, V., Gambardella, C., Garaventa, F., Drobne, D., Faimali, M., 2013. Effects of nano carbon black and single-layer graphene oxide on settlement, survival and swimming behaviour of *Amphibalanus amphitrite* larvae. *Chem. Ecol.* 29, 643–652. doi:10.1080/02757540.2013.817563

Moreira, S.M., Lima, I., Ribeiro, R., Guilhermino, L., 2006. Effects of estuarine sediment contamination on feeding and on key physiological functions of the polychaete *Hediste diversicolor*: Laboratory and in situ assays. *Aquat. Toxicol.* 78, 186–201. doi:10.1016/j.aquatox.2006.03.001

Moschino, V., Nesto, N., Barison, S., Agresti, F., Colla, L., Fedele, L., Da Ros, L., 2014. A preliminary investigation on nanohorn toxicity in marine mussels and polychaetes. *Sci. Total Environ.* 468–469, 111–9. doi:10.1016/j.scitotenv.2013.08.020

Mu, L., Gao, Y., Hu, X., 2016. Characterization of biological secretions binding to graphene oxide in water and the specific toxicological mechanisms. *Environ. Sci. Technol.* 50, 8530–8537. doi:10.1021/acs.est.6b02494

Oberdörster, E., Zhu, S., Blickley, T.M., McClellan-Green, P., Haasch, M.L., 2006. Ecotoxicology of carbon-based engineered nanoparticles: Effects of fullerene (C60) on aquatic organisms. *Carbon N. Y.* 44, 1112–1120. doi:10.1016/j.carbon.2005.11.008

Ohkawa, H., Ohishi, N., Yagi, K., 1979. Assay for lipid peroxides in animal tissues by thiobarbituric acid reaction. *Anal. Biochem.* 95, 351–358. doi:10.1016/0003-2697(79)90738-3

Pérez, E., Blasco, J., Solè, M., 2004. Biomarker responses to pollution in two invertebrate species: *Scrobicularia plana* and *Nereis diversicolor* from the Càdiz bay (SW Spain). *Mar. Environ. Res.* 58, 275–279. doi:10.1016/j.marenvres.2004.03.071

Petrone, N., Meric, I., Hone, J., Shepard, K.L., 2013. Graphene field-effect transistors with gigahertz-frequency power gain on flexible substrates. *Nano Lett.* 13, 121–125. doi:10.1021/nl303666m

Pires, A., Figueira, E., Moreira, A., Soares, A.M.V.M., Freitas, R., 2015. The effects of water acidification, temperature and salinity on the regenerative capacity of the polychaete *Diopatra neapolitana*. *Mar. Environ. Res.* 106, 30–41. doi:10.1016/j.marenvres.2015.03.002

Pires, A., Gentil, F., Quintino, V., Rodrigues, A.M., 2012. Reproductive biology of *Diopatra*

neapolitana (Annelida, Onuphidae), an exploited natural resource in Ria de Aveiro (Northwestern Portugal). *Mar. Ecol.* 33, 56–65. doi:10.1111/j.1439-0485.2011.00463.x

Potočnik, J., 2011. Commission recommendation of 18 October 2011 on the definition of nanomaterial (2011/696/EU). *Off. J. Eur. Union* 275, 38–40. doi:10.2777/13162

Pretti, C., Oliva, M., Pietro, R. Di, Monni, G., Cevasco, G., Chiellini, F., Pomelli, C., Chiappe, C., 2014. Ecotoxicity of pristine graphene to marine organisms. *Ecotoxicol. Environ. Saf.* 101, 138–45. doi:10.1016/j.ecoenv.2013.11.008

Rahman, S., Kim, K.-H., Saha, S.K., Swaraz, A.M., Paul, D.K., 2014. Review of remediation techniques for arsenic (As) contamination: A novel approach utilizing bio-organisms. *J. Environ. Manage.* 134, 175–185. doi:10.1016/j.jenvman.2013.12.027

Renn, O., Roco, M.C., 2006. Nanotechnology and the need for risk governance. *J. Nanoparticle Res.* 8, 153–191. doi:10.1007/s11051-006-9092-7

Sanchez, V.C., Jachak, a, Hurt, R.H., Kane, a B., 2012. Biological interactions of Graphene-Family Nanomaterials–an interdisciplinary review. *Chem. Res. Toxicol.* 15–34. doi:10.1021/tx200339h.Biological

Schniepp, H.C., Li, J., Mcallister, M.J., Sai, H., Herrera-alonso, M., Adamson, D.H., Prud, R.K., Car, R., Saville, D. a, Aksay, I. a, 2006. Functionalized single graphene sheets derived from splitting graphite oxide. *J. Phys. Chem B.* 2, 8535–8539. doi:10.1021/jp060936f

Shen, J., Hu, Y., Shi, M., Lu, X., Qin, C., Li, C., Ye, M., 2009. Fast and facile preparation of graphene oxide and reduced graphene oxide nanoplatelets. *Chem. Mater.* 21, 3514–3520. doi:10.1021/cm901247t

Solé, M., Kopecka-Pilarczyk, J., Blasco, J., 2009. Pollution biomarkers in two estuarine invertebrates, *Nereis diversicolor* and *Scrobicularia plana*, from a Marsh ecosystem in SW Spain. *Environ. Int.* 35, 523–531. doi:10.1016/j.envint.2008.09.013

Sun, T.Y., Bornhöft, N.A., Hungerbühler, K., Nowack, B., 2016. Dynamic probabilistic modeling of environmental emissions of engineered nanomaterials. *Environ. Sci. Technol.* 50, 4701–4711. doi:10.1021/acs.est.5b05828

Vonk, J. a, Struijs, J., van de Meent, D., Peijnenburg, W., 2009. Nanomaterials in the aquatic environment□: toxicity , exposure and risk assessment. 25. doi:RIVM Report 607794001/2009

Wang, D., Wang, J., Liu, Z.-E., Yang, X., Hu, X., Deng, J., Yang, N., Wan, Q., Yuan, Q., 2015. High-performance electrochemical catalysts based on three-dimensional porous architecture with conductive interconnected networks. *ACS Appl. Mater. Interfaces.* doi:10.1021/acsami.5b08294

Wu, Q., Yin, L., Li, X., Tang, M., Zhang, T., Wang, D., 2013. Contributions of altered permeability of intestinal barrier and defecation behavior to toxicity formation from graphene oxide in nematode *Caenorhabditis elegans*. *Nanoscale* 5, 9934–43. doi:10.1039/c3nr02084c

Yang, S.T., Wang, X., Jia, G., Gu, Y., Wang, T., Nie, H., Ge, C., Wang, H., Liu, Y., 2008. Long-term accumulation and low toxicity of single-walled carbon nanotubes in intravenously exposed mice. *Toxicol. Lett.* 181, 182–189. doi:10.1016/j.toxlet.2008.07.020

Yin, Z., Zhu, J., He, Q., Cao, X., Tan, C., Chen, H., Yan, Q., Zhang, H., 2014. Graphene-Based materials for solar cell applications. *Adv. Energy Mater.* 4, 1–19. doi:10.1002/aenm.201300574

Zhang, X., Hu, W., Li, J., Tao, L., Wei, Y., 2012. A comparative study of cellular uptake and cytotoxicity of multi-walled carbon nanotubes, graphene oxide, and nanodiamond. *Toxicol. Res. (Camb).* 1, 62. doi:10.1039/c2tx20006f

Zhang, Y., Mo, G., Li, X., Zhang, W., Zhang, J., Ye, J., Huang, X., Yu, C., 2011. A graphene modified anode to improve the performance of microbial fuel cells. *J. Power Sources* 196, 5402–5407. doi:10.1016/j.jpowsour.2011.02.067

Zhao, J., Wang, Z., White, J.C., Xing, B., 2014. Graphene in the aquatic environment□: adsorption , dispersion , toxicity and transformation. *Environ. Sci. Technol.* 48 (17), 9995–10009.

Zhou, X., Laroche, F., Lamers, G.E.M., Torraca, V., Voskamp, P., Lu, T., Chu, F., Spaink, H.P., Abrahams, J.P., Liu, Z., 2012. Ultra-small graphene oxide functionalized with polyethylenimine (PEI) for very efficient gene delivery in cell and zebrafish embryos. *Nano Res.* 5, 703–709. doi:10.1007/s12274-012-0254-x

Figure 1. **A:** Micro-IR spectrum of the as synthesized GO sample measured with the diamond anvil cell setup; **B:** IR spectra of representative GO in as synthesized water samples (purple); blank solution (red); PP sample point 1 (pink); PP sample point 2 (green). Point 1 displays evidence of $CaCO_{3;}$ Point 2 shows a sizeable organic fraction, with –NH, amide I and amide II bands vibrations (proteins). **C:** Micro-Raman spectra of: as synthesized GO and GO aggregates from (red); blank solution (blue); sample WP (green); and sample PP (dark yellow)

Figure 2. Scanning electron micrographs of GO artificial seawater dispersions drop-casted onto SiO_2/Si substrates. The thickness of the silicon oxide layer underneath was 280 nm. Scale bars are indicated in each panel. **A-B:** White arrows indicate sub-µm structures, isolated on the substrate and nicely distinguishable from other much larger structures. **C-E:** Details of nanoscale structures, characterized by very weak contrast and relatively sharp edges and angles (C-E).

Figure 3. Regenerative capacity of *Diopatra neapolitana* at 25 (left) and 53 (right) days after amputation, exposed to different GO concentrations (0.00; 0.01; 0.10 and 1.00 mg/L)

Figure 4. **A:** Glycogen (GLY) content; **B:** electron transport system (ETS) activity (mean + standard deviation), in *Diopatra neapolitana* exposed to different GO concentrations (0.00; 0.01; 0.10 and 1.00 mg/L). Different letters represent significant differences ($p \leq 0.05$) among GO concentrations

Figure 5. **A:** Lipid peroxidation (LPO) levels; **B:** GSH/GSSG ratio (mean + standard deviation), in *Diopatra neapolitana* exposed to different GO concentrations (0.00; 0.01; 0.10 and 1.00 mg/L). Different letters represent significant differences ($p \leq 0.05$) among GO concentrations

Figure 6. **A:** Superoxide dismutase (SOD) activity; **B:** Catalase (CAT) activity; **C:** Glutathione S-transferases (GSTs) activity (mean + standard deviation), in *Diopatra neapolitana* exposed to different GO concentrations (0.00; 0.01; 0.10 and 1.00 mg/L). Different letters represent significant differences ($p \leq 0.05$) among GO concentrations

Figure 7. Centroids ordination diagram (PCO) based on physiological and biochemical parameters, measured in *Diopatra neapolitana* exposed to different GO concentrations (0.00; 0.01; 0.10 and 1.00 mg/L). Pearson correlation vectors are superimposed as supplementary variables, namely physiological and biochemical data ($r > 0.75$): (CAT) Catalase activity; (GLY) Glycogen content; (ETS) Electron Transport System activity; (GSH/GSSG) GSH and GSSG ratio; (GSTs) Glutathione S-transferase activity; (LPO) Lipid Peroxidation levels; (SOD) Superoxide Dismutase activity; regeneration days (number of days need to complete the regeneration); new chaetigers (number of regenerated chaetigers at the end of the regeneration)

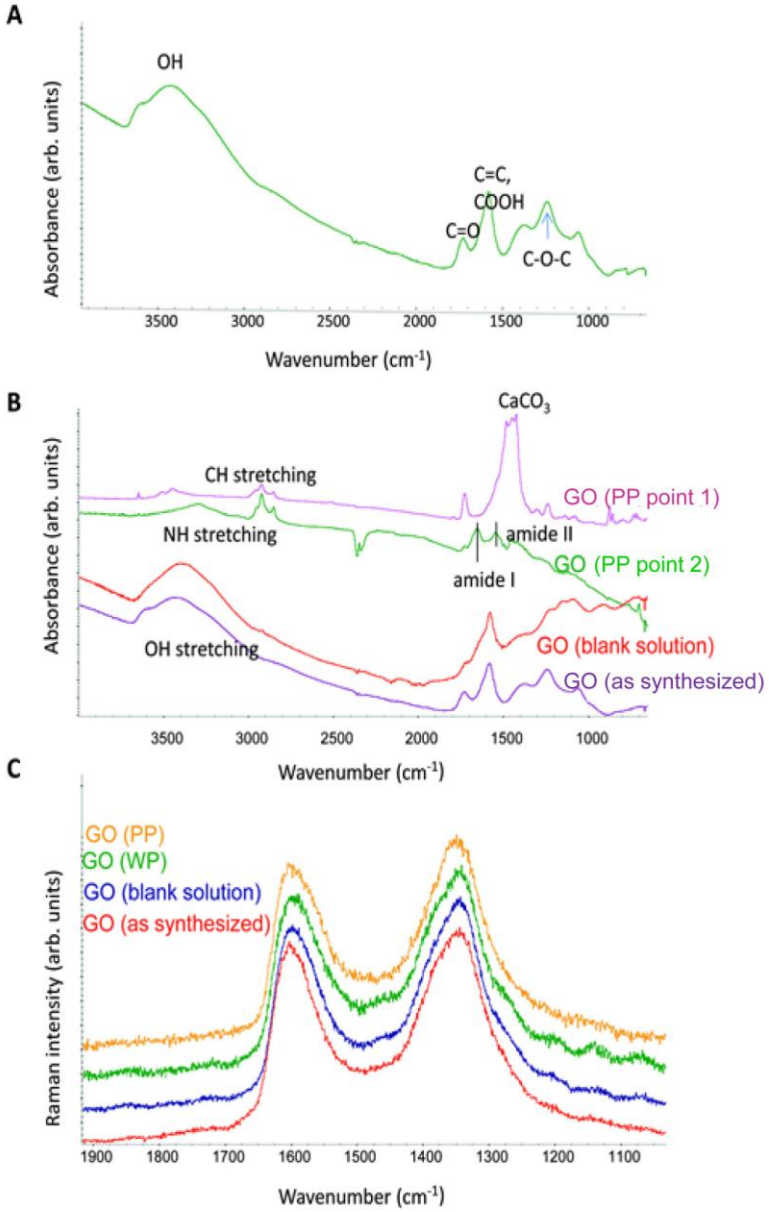

Fig. 1

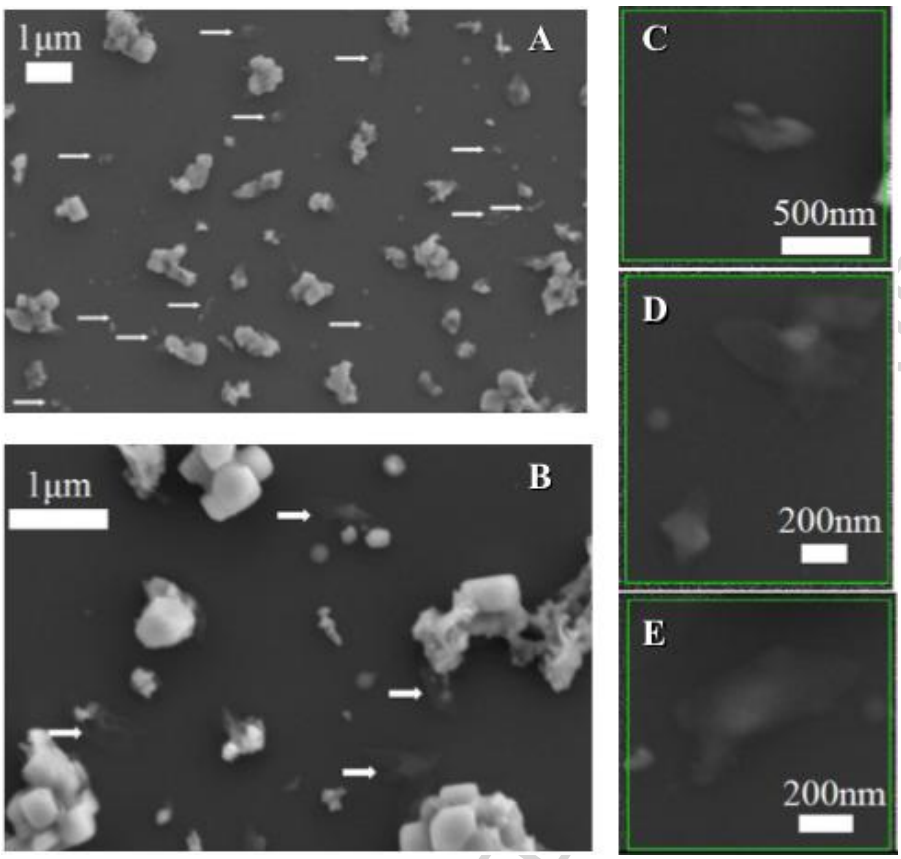

Fig. 2

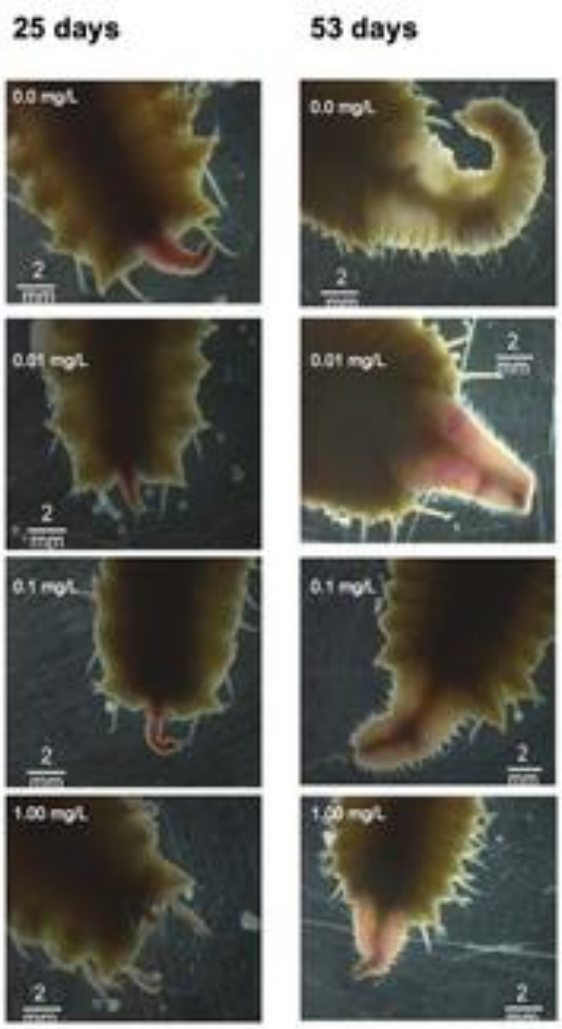

Fig. 3

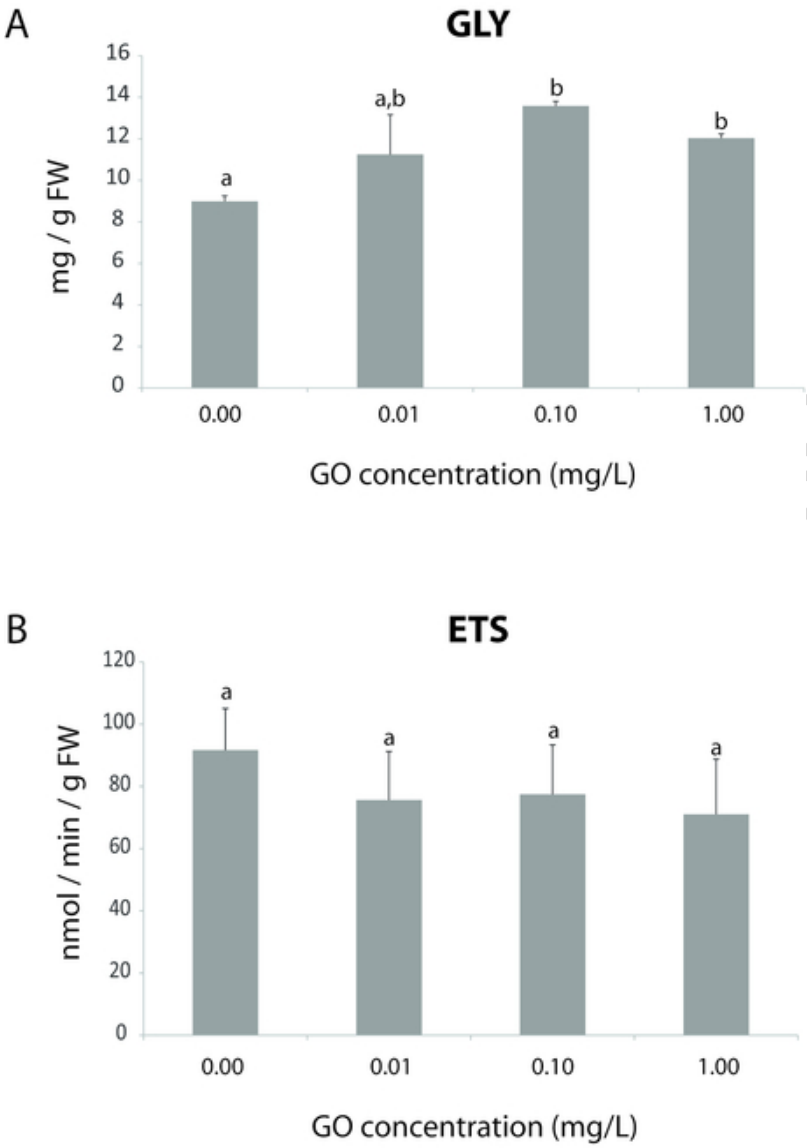

Fig. 4

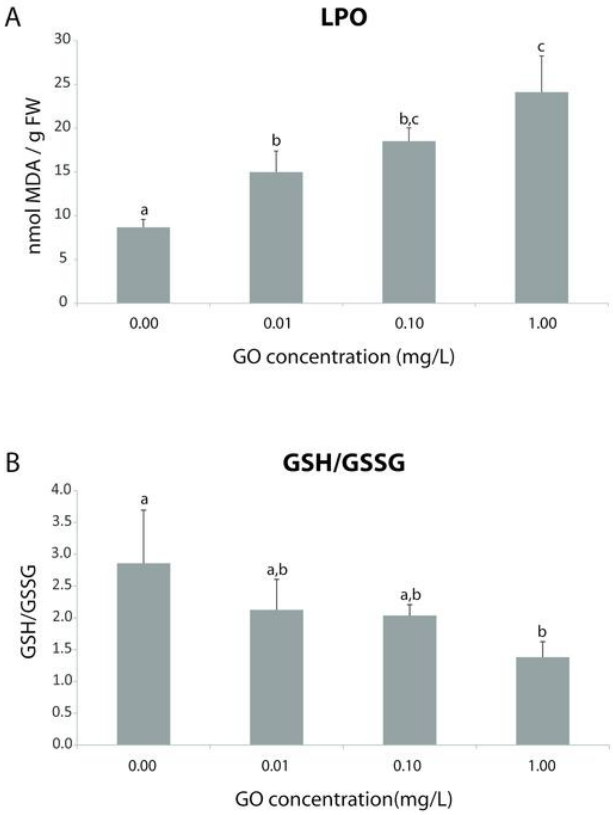

Fig. 5

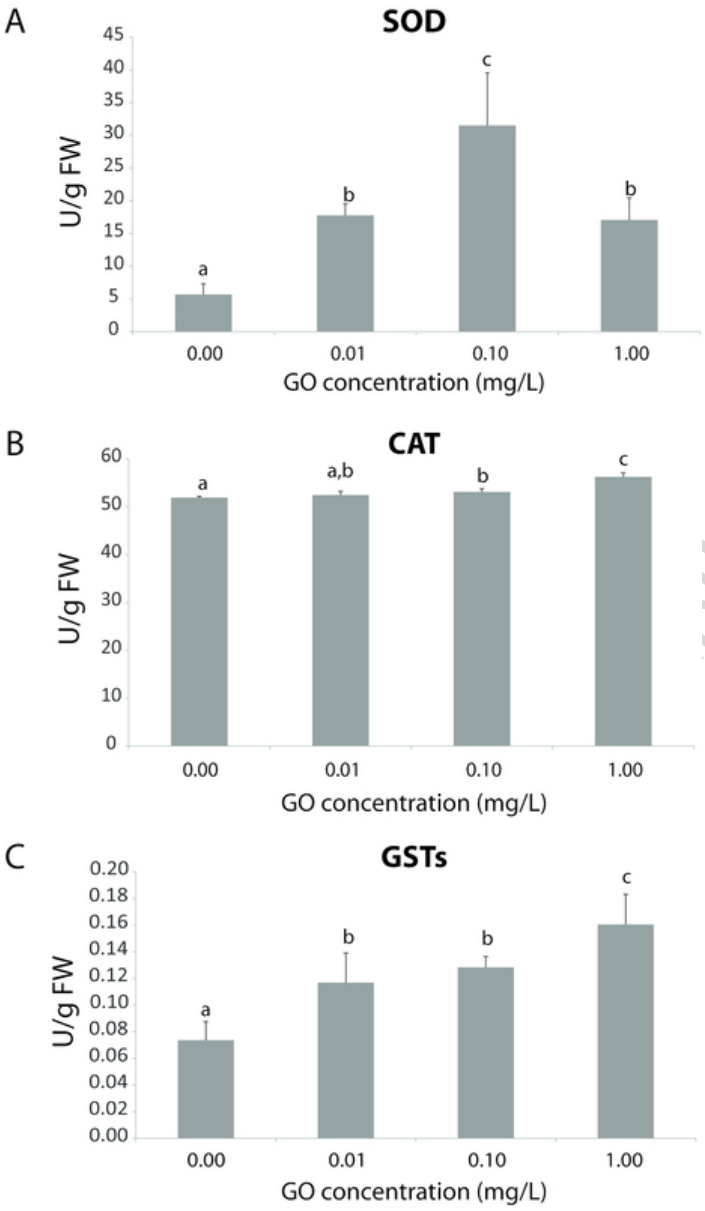

Fig. 6

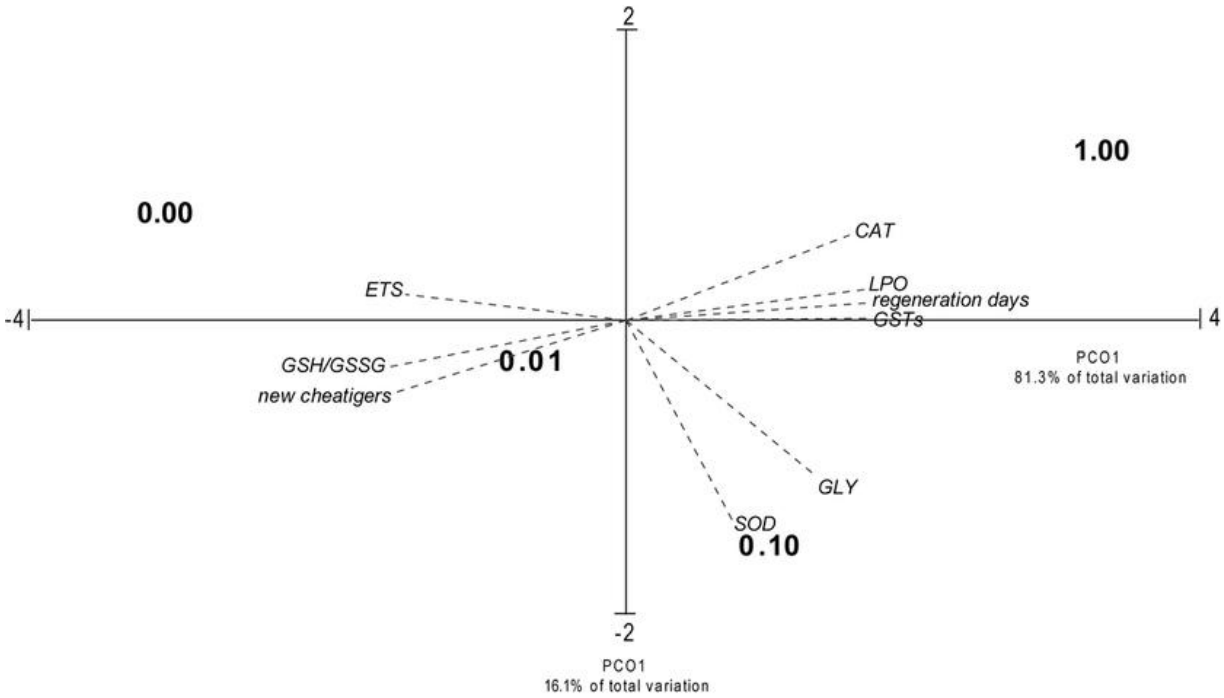

Fig. 7

Table 1. *Diopatra neapolitana* regenerative capacity

Regeneration period		GO concentrations (mg/L) 0.00	0.01	0.10	1.00
11 days	% body width	9.04±5.92 [a]	6.35±3.30 [a]	7.88±5.10 [a]	9.75±3.19 [a]
18 days	% body width	20.67±3,48 [a]	20.08 ±4.70 [a]	20.85±7.76 [a]	10.25±4.06 [a]
25 days	% body width	24.34±7.73 [a]	22.06±7.18 [a]	20.88±5.70 [a]	20.26±6.07 [a]
	# chaetigers	8.66±2.30 [a]	1.87±1.48 [a]	1.50±1.24 [a]	0±0 [b]
32 days	% body width	45.84±4.08 [a]	30.94±5.87 [a]	29.52±4.45 [a]	25.79±6.80 [b]
	# chaetigers	24.33±4.53 [a]	14.50±5.05 [a,b]	11.75±1.01 [a,b]	6.71±2.84 [b]
39 days	% body width	49.58±7.74 [a]	47.62±4.14 [a]	44.59±5.68 [b]	38.84±2.52 [b]
	# chaetigers	29.11±8.47 [a]	24.12±6.66 [a]	16.75±4.95 [b]	6.92±3.92 [b]
46 days	% body width	72.52±6.33 [a]	63.11±5.12 [b]	60.78±8.99 [b,c]	51.52±4.89 [c]
	# chaetigers	29.88±2.75 [a]	25.62±5.57 [a]	21.00±6.82 [b]	16.00±3.36 [b]
53 days	% body width	82.47±6.47 [a]	73.78±8.84 [b]	63.74±5.01 [b,c]	18.57±3.30 [c]
	# chaetigers	35.44±3.50 [a]	31.50±2.50 [b]	22.25±7.68 [c]	18.57±3.30 [c]
60 days	% body width	98.72±0.72 [a]	86.83±1.06 [b]	74.58±4.52 [b,c]	67.34±6.96 [c]
	# chaetigers	38.44±4.03 [a]	32.87±3.56 [a]	24.62±3.50 [b]	22.00±3.36 [c]
Complete regeneration	# days	62.00±1.73 [a]	68.50± 1.51 [b]	76.12±2.23 [c]	85.28 ±3.63 [d]
	# chaetigers	38.44±4.03 [a]	35.37±4.84 [a]	32.12±4.15 [a]	22.57±5.38 [b]

Regeneration data (% body width - percentage of regenerated body; # chaetigers - number of regenerated chaetigers) for *Diopatra neapolitana*, 11, 18, 25, 32, 39, 46, 53 and 60 days after amputation. The number of days needed to achieve full regeneration and the total number of new chaetigers after completed regeneration are also presented. Different letters (a-d) represent significant differences ($p \leq 0.05$) among conditions (0.00; 0.01; 0.10 and 1.00 mg/L GO).